

# Numerical Study on Onset Condition of Scour Below Offshore Pipeline Under Reversing Tidal Flow

**Zhiyong Zhang\***

1. Zhejiang Institute of Hydraulics and Estuary, 50 Fengqidong Road, Hangzhou, China
2. Zhejiang Provincial Key Laboratory of Estuary and Coast, 50 Fengqidong Road, Hangzhou, China.
3. Zhejiang Institute of Marine planning and design, 50 Fengqidong Road, Hangzhou, China.

e-mail: 82457114zzy@163.com

**Yuanping Yang**

1. Zhejiang Institute of Hydraulics and Estuary, 50 Fengqidong Road, Hangzhou, China
2. Zhejiang Provincial Key Laboratory of Estuary and Coast, 50 Fengqidong Road, Hangzhou, China
3. Zhejiang Institute of Marine planning and design, 50 Fengqidong Road, Hangzhou, China

## ABSTRACT

It is important to study the onset condition of scour below offshore pipelines for the protection of pipeline. In this paper a new and small scale numerical reversing tidal flow flume is established using FLOW-3D Software. This numerical flume can simulate the time process of tidal level as well as the flow velocity and shows good reliability. Using this numerical flume, the onset condition of scour below offshore pipelines under reversing tidal flow is discussed. The flow fields at different times in a period are analyzed and the influences of middle tidal level, flow velocity and buried depth on pressure difference are studied systematically. The onset condition of scour below offshore pipeline for reversing tidal flow is determined, which supplies the technical support for practical engineering.

**KEYWORDS:** reversing tidal flow; offshore pipeline; numerical flume; onset condition

## INTRODUCTION

Offshore pipeline, which transfers oil or gas from offshore to onshore, is one of the most important marine engineering equipment. As for the offshore pipelines laid directly on sandy seabed, the complex marine hydrodynamic conditions often induce the local scour below pipeline and cause suspension, which makes the offshore pipeline unstable and have potential risk of fracture.

Consequently, understanding the problem of local scour below offshore pipeline has its importance for pipeline designs and operations.

At present, there are numerous studies on local scour below offshore pipelines. Most of the studies focused on the local scour under unidirectional steady flow or wave, The work on local scour under unidirectional steady flow can be found in (Mao 1986; Sumer et al. 1988; Chiew 1991; Bros 1999; Li and Cheng 2001; Liang and Cheng 2004; Lu et al.2005; Zhao and Fernando 2007; Dey and Singh 2008; Wu and Chiew 2012; Yang et al. 2012; Yang et al.2014; ),and the work on local scour under short period wave action can be found in (Sumer and Fredsoe 1990; Cevic and Yuksel 1999; Pu et al. 2001; Xu et al. 2010; Yasa 2011; Kazaminezhad et al. 2012).As for the scour mechanism below offshore pipeline ,Chiew (1990) conducted a series of physical experiments and found that piping is the main factor for the initiation of scour. Under unidirectional flow, the pipeline disturbs the flow and makes large pressure difference between upstream and downstream sides of pipeline (Fig.1), which induces seepage flow in the sandy seabed and seepage force on soil particles. When the pressure gradient at the exit of seepage flow (Point B in Fig.1) exceeds the floatation pressure gradient, sand particles start moving downstream and scour take places. Sumer et al. (2001) studied the onset of scour below pipelines under steady flows or waves by laboratory experiments. They measured the pressures on the surface of a partially buried pipeline at two points (Point A and B in Fig.1) in the seabed and the critical velocity for the onset of scour under flows/waves was obtained. Zang et al. (2009) developed a numerical model to predict the onset condition of scour in flows/waves. They studied the relation between the average pressure gradient from upstream contact point A to downstream point B and the maximum pressure gradient at the exit of seepage flow in the seabed by solving the Darcy's law. By assuming that the scour starts when the maximum pressure gradient exceeds the floatation gradient of sediment, the onset condition of scour was obtained and a scour onset expression in waves was proposed. Zhang et al. (2013) established a new numerical model to simulate the seepage flow by assuming the seabed as porous media and adding source terms in momentum equations. Using this model, they discussed the influence of impermeable plate below pipeline on the seepage flow under steady flow and gave the critical length of plate for preventing scour.

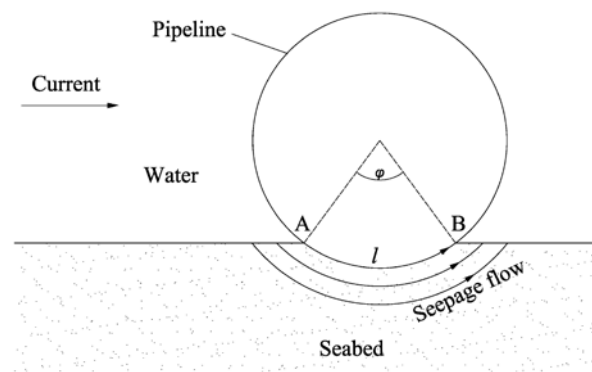


**Figure 1:** Schematic diagram of Seepage flow around pipeline

Although the previous work has given the onset condition of scour below pipeline under steady flows or waves, there is still no work on the flow field and onset condition of scour under reversing tidal flow. In practical engineering, the tidal flow in the ocean often changes with the tidal level. Especially in the near shore region, the tidal flow is reversing. Fig.2 shows the typical time process of tidal flow and tidal level near Cezhen Oil Pipeline in Hangzhou Bay, China. It can be seen that the period of tide is about 12 hours which is more larger than short period waves and the phase lag between flow and tidal level is about  $\pi/2$ . The flow reverses the flow direction in a tidal cycle and tidal velocity nearly reaches to the maximum value when the water level is middle tidal level, while the velocity is close to zero when the tidal level is high tidal level or low tidal level. Variations of flow velocity and tidal level may cause significant differences in flow field and onset condition of scour compared with the cases under steady flow.

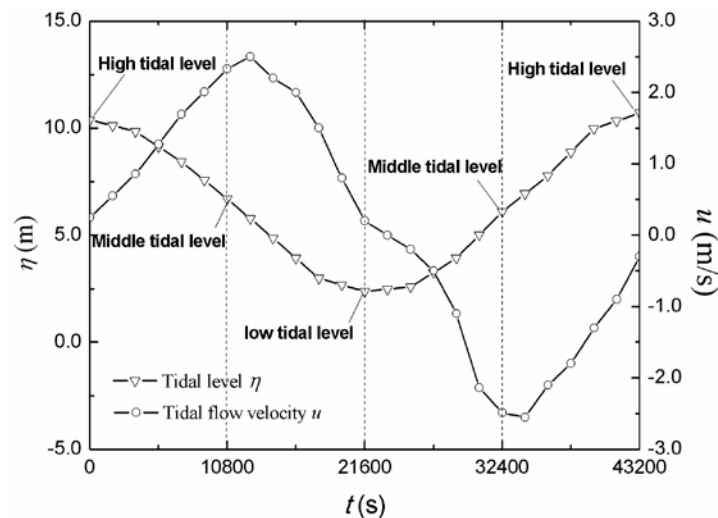


**Figure 2:** Time processes of tidal level and tidal flow velocity

To study the flow and onset condition of scour below pipeline under reversing tidal flow, a reversing tidal flow flume should be firstly established. However the flow velocity and water depth must be regulated simultaneously, which makes the flume difficult to be established in laboratory. In recent years, with the development of computing technology and numerical models, many kinds of numerical water flume, such as numerical wave flume, numerical wave and flow flume, have been developed as effective tools to study relative problems due to the advantages of low cost, no scale issue and full information. FLOW-3D is a famous CFD software in the world, and it is skilled in fluid simulation, especially the problems considering the change of fluid surface. Based on FLOW-3D, a new numerical reversing tidal flow flume considering water surface change is developed. The flow fields around pipeline under reversing tidal flow at different times in a period are simulated. The influences of middle tidal level, maximum flow velocity and buried depth on pressure difference are discussed systemically, and finally the onset condition of scour below pipeline under reversing tidal flow is obtained.

## NUMERICAL MODEL

### GOVERNING EQUATIONS

FLOW-3D solves the Navier-Stokes equations and continuity equation with a free boundary. The continuity equation (1) and Reynolds-averaged Navier-Stokes equations (2) can be expressed as

$$\frac{\partial v_i A_i}{\partial x_i} = 0 \quad (1)$$

$$\frac{\partial v_i}{\partial t} + \frac{1}{V_f} (v_j A_j \frac{\partial v_i}{\partial x_j}) = -\frac{1}{\rho} \frac{\partial P}{\partial x_i} + G_i + f_i \quad (2)$$

where  $v_i$  is the mean velocity,  $A_i$  is the fraction open area in the  $i$  direction,  $V_f$  is the fraction volume open to flow,  $P$  is the pressure,  $G_i$  represents the gravity acceleration,  $f_i$  represents the viscous acceleration.

The momentum equation should be closed by turbulence model. In this paper, we choose the standard  $k-\varepsilon$  model which has been used to simulate the flow field around pipeline in previous work (Smith and Foster 2005).

Volume of Fluid (VOF) method (Hirt and Nichols 1981) is used to capture the fluid-air or fluid-fluid sharp interfaces in FLOW-3D. The volume of fluid in each cell is recorded and compared to surrounding cell volumes to determine slope and curvature of fluid with the cell.

FLOW-3D also offers a new technique called Fractional Area-Volume Obstacle Representation (FAVOR) method (Flow Science 2010) to capture the solid boundary. This method allows rectangular grids to be set up without distorting the properties of an obstacle in computational region. This method calculates open cell areas and volumes to define the region within the cell which is occupied by the obstacle.

## MODEL SETUP

As for the research in this paper, a vertical two dimensional numerical flume is established and the computational domain is shown in Fig.3. The left boundary was set as pressure condition and the time processes of flow velocity in  $x$  direction and tidal level are given to the boundary. The velocity condition is defined at right boundary and the time processes of flow velocity and tidal level are the same as the values at left boundary. The symmetry boundary is used at upper boundary and the lower boundary which represents seabed is set as wall boundary. The pipe located at a distance of  $20D$  (2m) ( $D$  is pipe diameter, here  $D=0.1$ m) from both the left and right boundary. The vertical distance is 1.2

$\eta_{max}$  ( $\eta_{max}$  is high tidal level). The whole computational domain is discretized using rectangular meshes.

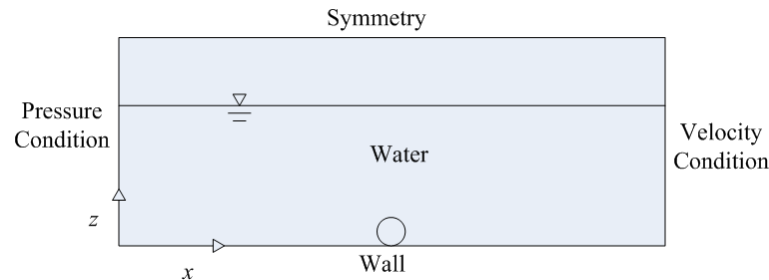


**Figure 3:** Computational domain

## MODEL VALIDATION

To validate the efficiency of numerical reversing tidal flow flume, one case without pipeline is simulated. This case selects the regular tidal flow and tidal level which can be express as

$$u = u_{max} \sin(2\pi t / T) \quad (3)$$

$$\eta = \eta_0 + \frac{H}{2} \sin(2\pi t / T + \pi / 2) \quad (4)$$

where  $T$  is tidal period,  $\eta_0$  is middle tidal level, and  $H$  is tidal range,  $H = \eta_{max} - \eta_{min}$ ,  $\eta_{max}$  and  $\eta_{min}$  are high and low tidal level respectively. In this case, the parameters in Eq(3) and Eq.(4) are selected as follows,  $T=480s$ ,  $u_{max}=0.8m/s$ ,  $\eta_0=0.5m$ , and  $A=0.4m$ .

The numerical model was run one tidal period for each case. The simulation result at cross-section  $x=2m$  was used for the comparison of tidal level, and the horizontal velocity at point  $x=2m, z=\eta_{min}/2$  was used for the comparisons of flow velocity. Fig.4 shows the comparisons of simulated and expected tidal levels and velocities. It can be seen that there is a good agreement between numerical results and expected results, which implies present numerical reversing tidal flow flume well simulates the expected time processes of tidal level and flow velocity.

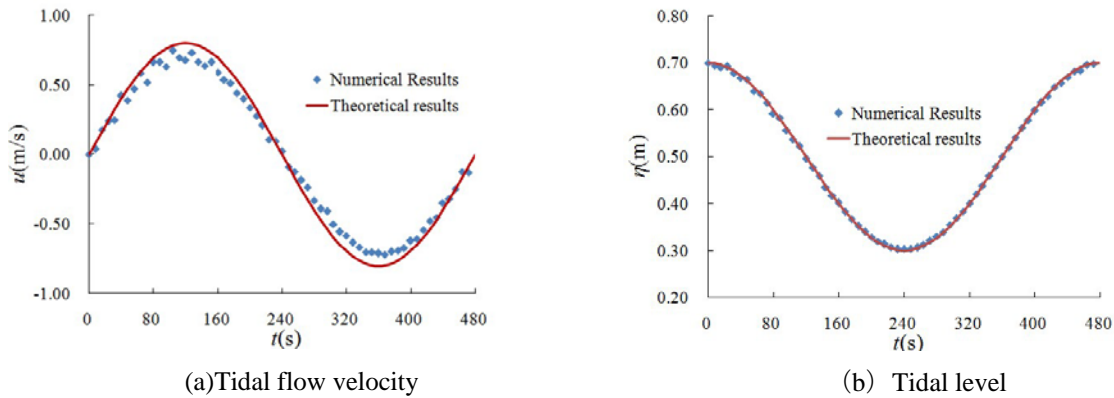


**Figure 4:** Comparisons of numerical and theoretical results of tidal level and flow velocity

## RESULTS AND DISCUSSIONS

As has been shown in Fig.1, the pressure difference between upstream and downstream sides of pipeline is the domain factor for seepage flow and piping. The pressure difference can be obtained by

$$\Delta P = P_A - P_B \quad (5)$$

where  $P_A$  is the pressure at point A,  $P_B$  is the pressure at point B.

The non-dimensional pressure coefficient can be expressed as

$$\Delta C_p = \frac{\Delta P}{0.5 \rho u_{\max}^2} \quad (6)$$

According to the formula in previous article (Zang et al.,2009), the scour under offshore pipeline in reversing tidal flow happens when the non-dimensional velocity  $u_{\max}^2 / (gD(s-1)(1-n))$  fulfills the following equation

$$\frac{u_{\max}^2}{gD(s-1)(1-n)} \geq V_{cr} \quad (7)$$

$$V_{cr} = \frac{\varphi}{\lambda \Delta C_{p \max}} \quad (8)$$

where  $V_{cr}$  is the non-dimensional critical velocity for onset of scour.  $\varphi$  is the contact angle of buried part of pipe (Fig.1),  $\lambda$  is a calibration coefficient which represents the relation between the maximum pressure gradient at exit of seepage and average pressure gradient,  $\lambda = 3.0 \exp(-0.42e / D)$ ,  $s$  is

relative density of sediment,  $n$  is sediment porosity.  $\Delta C_p^{max}$  is the maximum value of pressure difference coefficient  $\Delta C_p$  in a tidal period.

From Eq.(8), most of these parameter can be obtained except for  $\Delta C_p^{max}$ , consequently the determination of pressure difference  $\Delta C_p$  and  $\Delta C_p^{max}$  will be discussed in the following sections.

Tab.1 lists the ranges of parameters of simulation cases. All the cases select the regular tidal flow velocity and level which can be obtained by Eq.(3) and Eq.(4) respectively.

**Table 1:** Parameters range of computational cases

Tidal period $T(s)$	Pipeline diameter $D(m)$	Maximum tidal flow velocity $u_{max}(m/s)$	middle tidal level $\eta_0/D$	tidal range $H/D$	buried depth $e/D$
480,43200	0.1	0.3,0.5,0.8	3.0,4.0,5.0,6.0,7.0	3.0,4.0,6.0	0.0, 0.01, 0.1, 0.3, 0.5, 0.8

### TIME PROCESS OF $\Delta C_p$

The pressure difference over the pipeline  $\Delta C_p$  is obtained by extracting the pressure data from simulation results. Fig.5 shows the time process of pressure difference coefficient  $\Delta C_p$ . It can be found that  $\Delta C_p$  is positive when tidal current flows from left to right, while  $\Delta C_p$  turns to negative value when tidal current flows from right to left, which induces reversing seepage flow in the seabed. Besides it can also be found that there is a very small phase difference between  $\Delta C_p$  and velocity  $u$ , and the maximum pressure difference  $\Delta C_p^{max}$  occurs when the tidal level is a little lower than middle tidal level.

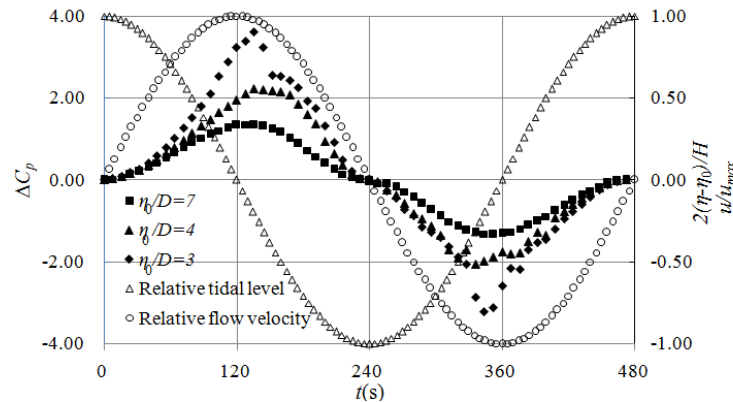


**Figure 5:** Time process of  $\Delta C_p$  versus relative tidal level and flow velocity

## EFFECT OF TIDAL PERIOD

In many estuaries, the tide is often half-day tide. The computer needs to run one week for calculating a tidal period of 12 hours, which is very time-consuming. During the simulation, we found that the pressure differences  $\Delta C_p$  when  $T=480s$  are closer to the results in case of  $T=43200s$  and the maximum pressure differences  $\Delta C_p^{max}$  are also closer, which has been shown in Fig.6. As such, to save computational time, the tidal periods of following computational cases are all the same and  $T=480s$ .

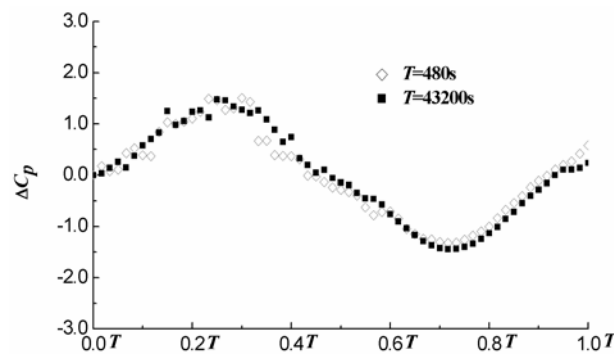


**Figure 6:** Time processes of  $\Delta C_p$  in different  $T$

## EFFECT OF TIDAL FLOW VELOCITY

The effect of tidal flow velocity on pressure difference is achieved by adjusting the maximum tidal velocity  $u_{max}$ . Fig.10 shows the time processes of pressure difference coefficients  $\Delta C_p$  in different velocities. Seen from Fig.7, the variations of  $\Delta C_p$  are nearly the same and maximum pressure difference  $\Delta C_p^{max}$  are in agreement with each other which implies that the effect of tidal flow velocity on  $\Delta C_p$  is weak.

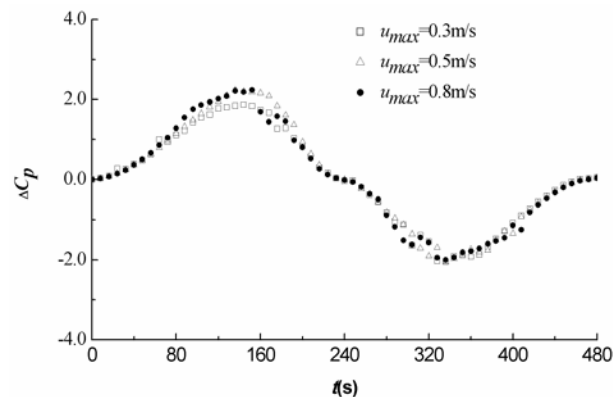


**Figure 7:** Time processes of  $\Delta C_p$  in different  $u_{max}$

## EFFECT OF MIDDLE TIDAL LEVEL

As has been shown in Fig.8, the maximum pressure differences are different in cases of different middle tidal level  $\eta_0/D$ . Figure 11 illustrates the relation between the maximum pressure difference  $\Delta C_p^{max}$  and  $\eta_0/D$ . The pressure difference in case of unidirectional steady current is also shown in Fig.11. Considering the variation of water free surface, pressure difference consist two parts: One is the static pressure caused by the water level difference over pipeline, another is from the dynamic pressure induced by the variation of velocity. When  $\eta_0/D$  is shallower, the blockage effect is more significant and the water level difference over pipeline is larger. As such, the maximum pressure difference  $\Delta C_p^{max}$  decreases with the increasing  $\eta_0/D$ . When  $\eta_0/D$  is larger than 5.0,  $\Delta C_p^{max}$  reaches to a nearly steady value, which illustrates that there is no noticeable change of the water surface and  $\Delta C_p^{max}$  is independent of  $\eta_0/D$  when  $\eta_0/D$  is larger than 5.0. By comparing the numerical results under reversing tidal flow with the experimental results under steady current,  $\Delta C_p^{max}$  under reversing tidal flow is a little larger than the results in steady current when the water level in steady current equals to the middle tidal level. This may be because that the maximum pressure difference occurs when the tidal level is a little smaller than middle tidal level and the blockage effect will be more significant. Consequently,  $\Delta C_p^{max}$  at that time will be larger than the one in middle tidal level.

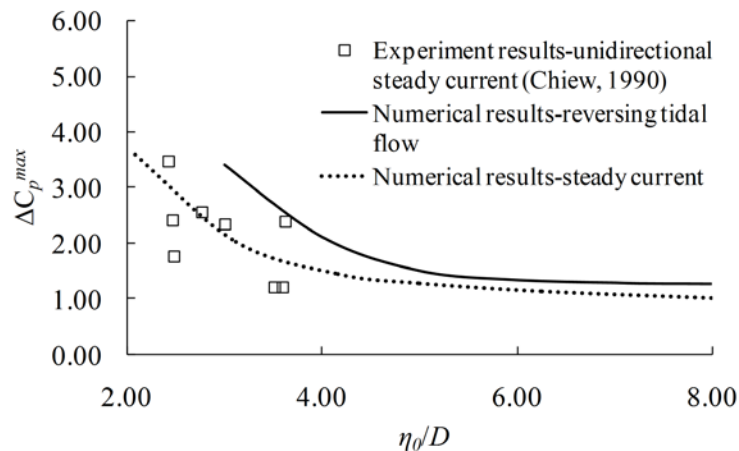


**Figure 8:** Variations of  $\Delta C_p^{max}$  with  $\eta_0/D$ ,  $e/D=0$

## EFFECT OF BURIED DEPTH

Sumer et al. (2001) found that the piping potential decreases as the pipeline buried depth increases. In the present study, the buried depth  $e/D$  ranges from 0.0 to 0.8 are investigated. The maximum pressure difference coefficients  $\Delta C_p^{max}$  are calculated in three different middle tidal levels, namely  $\eta_0/D=3, 4, 5$  and 7 in Fig.9. It can be seen that  $\Delta C_p^{max}$  decreases with the increase of buried depth  $e/D$  in three cases, and with the increasing of middle tidal level,  $\eta_0/D$ , the reducing rate of  $\Delta C_p^{max}$  decreases owing to the weakening of the blockage effect until  $\eta_0/D$  reaching 5.0.

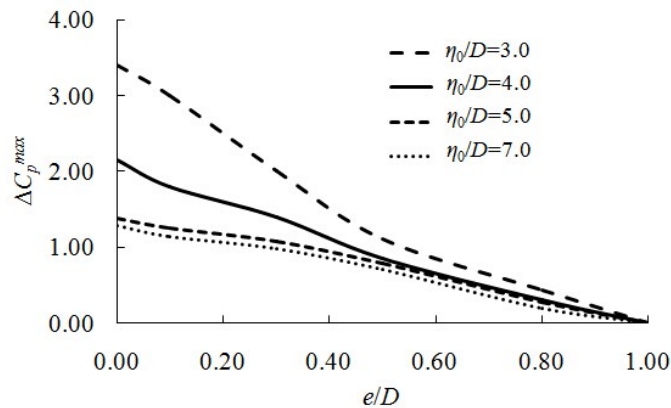


**Figure 9:** Variations of  $\Delta C_p^{max}$  with  $e/D$

## ONSET CONDITION

After the maximum pressure difference coefficients  $\Delta C_p^{max}$  are obtained by numerical model using Flow-3D software, the non-dimensional critical velocity  $V_{cr}$  can be obtained using Eq.(8). The variations of the critical onset velocity with buried depth  $e/D$  for  $\eta_0/D=3, 4, 5$  and  $7$  are shown in Fig. 10. It can be seen that with the increasing buried depth  $e/D$ , the non-dimensional critical velocity needed to initiate scour becomes larger. When the flow velocity is over the critical value, scour will happen. It can also be seen that for a given value of buried depth  $e/D$ , the non-dimensional critical velocity increases with increasing  $\eta_0/D$  owing to the blockage effect when  $\eta_0/D$  is smaller than  $5.0$ . When  $\eta_0/D$  is larger than  $5.0$ , the blockage effect is insignificant and the non-dimensional critical velocity is only dependent on buried depth. Besides, due to the larger  $\Delta C_p^{max}$ , the non-dimensional critical velocity under reversing tidal flow are smaller than that under steady current in the same water depth  $\eta_0/D$  and buried depth  $e/D$ .

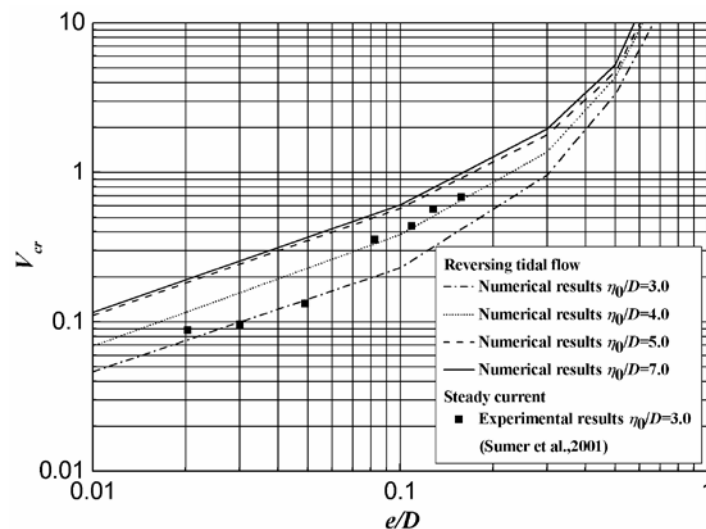


**Figure 10:** Variations of non-dimensional critical velocity with  $e/D$

## CONCLUSIONS

A numerical reversing tidal flow flume is established using FLOW-3D software. This numerical flume is determined by solving the Reynolds-averaged Navier-Stokes equations with a  $k-\varepsilon$  turbulence closure, and can simulate the time processes of tidal level and tidal current simultaneously. Using this numerical flume, the flow fields and pressure difference  $\Delta C_p$  around offshore pipeline in a tidal period are studied. Some conclusions can be drawn from this study:

1. In reversing tidal current, the blockage effect is significant and induce distinct water level difference over pipeline when middle tidal level is smaller than  $5.0D$ .

2. The effects of time period and maximum tidal velocity on pressure difference coefficient  $\Delta C_p$  under reversing tidal flow are weaken, and the maximum pressure difference  $\Delta C_p^{max}$  decreases with the increases of middle tidal level  $\eta_0/D$  and buried depth  $e/D$ .

3. In case of the reversing tidal flow, the critical condition for onset of scour is determined by three parameters, the middle tidal level  $\eta_0/D$ , the buried depth  $e/D$ , and the non-dimensional velocity  $V_{cr} = u_{max}^2 / (gD(s-1)(1-n))$ . The non-dimensional critical velocity  $V_{cr}$  increases with the increase of  $e/D$  and also increases with  $\eta_0/D$  until  $\eta_0/D$  reaching 5.0. It is independent on  $\eta_0/D$  if  $\eta_0/D$  is greater than 5.0. The onset condition of scour below offshore pipeline can be determined using Fig.10.

## ACKNOWLEDGEMENT

The authors would like to acknowledge the financial supports from the National Nature Science Fund of China (Grant No. 41376099) and Zhejiang province science and technology conditions of construction project (2014F10007, 2014F10036).

## REFERENCES

1. Brørs B,(1999) Numerical Modeling of Flow and Scour at Pipelines. J Hydraul Eng 125(5): 511-523
2. Cevi E, Yuksel Y,(1999) Scour under submarine pipelines in waves in shoaling conditions. J Waterw Port Coastal Ocean Eng 125(1):9-19
3. Chiew, YM,(1990) Mechanics of local scour around offshore pipelines. J Hydraul Eng 1990, 116(4): 452-466
4. Chiew YM,(1991) Prediction of maximum scour depth at submarine pipelines. J Hydraul Eng 117(4): 452-466
5. Dey S, Singh, NP,(2008) Clear-water scour depth below underwater pipelines under steady flow. J Hydraul Eng 134(5): 588-600

6. Flow Science, (2010) FLOW-3D User's Manual
7. Hirt CW, Nichols BD, (1981) Volume of Fluid (VOF) Method for the Dynamics of Free Boundaries. *J Comput Phys* 39,201-225
8. Kazeminezhad MH, Bakhtiary AY, Etemad-Shahidi A, (2012) Two-Phase Simulation of Wave-Induced Tunnel Scour beneath Marine Pipelines. *J Hydraul Eng* 138(6):517-529
9. Li FJ, Cheng L, (1999) A numerical model for local scour under offshore pipelines. *J Hydraul Eng* 125(4):400-406
10. Liang DF, Cheng L, Li FJ, (2004) Numerical modeling of scour below a pipeline in currents. part II: Scour simulation. *Coastal Eng* 52(1): 43-62
11. Lu L, Li YC, Qin JM, (2005) Numerical simulation of the equilibrium profile of local scour around submarine pipeline based on renormalized group turbulence model. *Ocean Eng* 32(17-18):2007-2019
12. Mao Y, (1986) The interaction between a pipeline and an erodible bed. Dissertation, Technical University of Denmark
13. Pu Q, Li K, Gao FP, (2001) Scour of the seabed under a pipeline in oscillating flow. *China Ocean Eng* 15(1):129-137
14. Smith HD, Foster DL, (2005) Modeling of flow around a cylinder over a scoured bed. *J Waterw Port Coastal Ocean Eng* 131(1):14-24
15. Sumer BM, Jensen HR, Fredsøe J, (1988) Effect of lee-wake on scour below pipelines in current. *J Waterw Port Coastal Ocean Eng* 114(5):599-614
16. Sumer BM, Fredsøe J, (1990) Scour below pipelines in waves. *J Waterw Port Coastal Ocean Eng* 116(3):307-323
17. Sumer BM, Truelsen C, Sichmann T, (2001) Onset of scour below pipelines and self-burial. *Coastal Eng*, 42:313-335
18. Wu YS, Chiew YM, (2012) Three-Dimensional Scour at Submarine Pipelines. *J Hydraul Eng* 138(9): 788-795
19. Xu JS, Li GX, Dong P, (2010) Bedform evolution around a submarine pipeline and its effects on wave-induced forces under regular waves. *Ocean Eng* 37:304-313
20. Yang, LP, Shi B, Guo YK, Wen XY, (2012) Calculation and experiment on scour depth for submarine pipeline with a spoiler. *Ocean Eng* 55:191-198
21. Yang LP, Shi B, Guo YK, Zhang LX, Zhang JS, Han Y, (2014) Scour protection of submarine pipelines using rubber plates underneath the pipes. *Ocean Eng* 84:176-182
22. Yasa R, (2011) Prediction of the Scour Depth under Submarine Pipelines in Wave Condition. *J Coastal Res* 64:627-630

23. Zang, Z.P., Cheng,L., Zhao, M., 2009. A numerical model for onset of scour below offshore pipelines. *Coastal Eng* 56:458–466
24. Zhang ZY, Shi B, Guo YK, Yang LP ,(2013) Numerical Investigation On Critical Length of Impermeable Plate Below Underwater Pipeline Under Steady Current. *Sci China: Technol Sci* 56(5):1232-1240
25. Zhao ZH, Fernando HJS, (2007) Numerical simulation of scour around pipelines using an Euler-Euler coupled two-phase model. *Environ Fluid Mech.* 7:121-142

